Effect of Model Potential of Adsorptive Bond on the Thermodynamic Properties of Adsorbed CO Molecules on Ni(111) Surface

Amir N. Shamkhali and Gholamabbass Parsafar*

Department of Chemistry and Nanotechnology Research Center, Sharif University of Technology, P.O. Box 11365-9516, Tehran, Iran

Received: March 14, 2006; In Final Form: July 9, 2006

The effect of anharmonicity on the adsorption of CO molecules on the Ni(111) surface has been investigated. The DFT calculations are used to obtain the effective adsorption potential of the CO molecule on the Ni(111) surface. First, using an appropriate slab model, the geometry of adsorption system corresponding to hcp, fcc, bridge, and on-top sites with p(2 × 2) arrangement and coverage of 0.25 ML is optimized by the DFT calculations using a plane wave basis set and ultrasoft pseudopotentials; this gives the hcp site as the most stable site with $D_e = 185$ kJ/mol, for which the equilibrium distance of CO from the surface and C−O bond length on the surface are found to be 1.31 and 1.192 Å, respectively. Then, the potential function of adsorption versus adsorptive bond distance was plotted, which is significantly different from that of a harmonic oscillator, i.e., the anharmonicity for the adsorptive bond is significant. Also the harmonic and anharmonic shifts of vibrational frequencies of adsorptive and C−O bonds are calculated to be −22.6 and 7.8 cm^{-1}, respectively. Hence, two potential models are selected for which their Schrödinger equations are solved analytically, namely the hard repulsion−soft attraction (HS) and Morse potential (MP) models. The adsorption isotherms, internal energy, isochoric heat capacity, and entropy of adsorbed CO molecules have been calculated for the mentioned model potentials and compared with those of the harmonic oscillator (H). As a result, the adsorption isotherms are not considerably sensitive to the model potential. The anharmonicity of CO−Ni bond, which is included in HS and MP models, gives an average deviation in pressure as much as 1.4% for HS and 5.8% for MP, compared to 6.1% for the H model. However, isochoric heat capacity and entropy depend on the model potential significantly, and the differences may be as high as 69% and 55% for isochoric heat capacity and entropy, respectively.

Introduction

Investigation of adsorption phenomena is mainly related to the study of vibration of adsorbed molecules on the surface. A simple approach for such an investigation is via classical statistical mechanics. However, because the separation of vibrational energy levels is too far apart to be treated classically, the classical treatment of vibrational degree of freedom is reasonable only at high temperatures.[1] Therefore, the accurate study of adsorption may be done by quantum statistical mechanics. However, the Schrödinger equation for many- body systems is too complicated to be solved analytically. Therefore, one may use a simple model like a harmonic oscillator to investigate such phenomena. However, the important aspect of a chemical bond is its anharmonic behavior. Anharmonicity leads to different trends for attraction and repulsion walls of the potential energy surface, which has effects on vibrational frequencies of chemical bonds and hence on vibrational partition functions. To take the anharmonic effect of the adsorptive bond into account, the following questions should be clarified: (1) How significant is the anharmonicity of the adsorptive bond? (2) Is it reasonable to ignore the anharmonic coupling of the adsorptive bond with other bonds? The answers to these questions may guide us to present appropriate models for adsorptive bond.

The effect of anharmonicity on adsorption phenomena was studied by different researchers for the adsorption of some simple molecules on transition metal surfaces. Loffreda et al. calculated N−O stretching frequencies for low coverage adsorption of NO on Pd_3Mn(100) and (111) surfaces using periodic DFT calculations.[2] They concluded that the frequencies depend both on the coordination of the site (hollow, bridge, etc.) and on the chemical nature of the metal atoms. Loffreda et al. also interpreted variation in N−O stretching frequencies for different sites of Pd_3Mn alloy using Mulliken population analysis.[2] Titmuss et al. studied structure, bonding, and anharmonic librational motion of CO molecules adsorbed on an Ir(100) surface by a combination of low-energy electron diffraction (LEED) technique and DFT calculations.[3] They concluded that the potential energy surface for librational motion of atop-CO in the p(2 × 2) phase is anharmonic and the harmonic potential energy surface local to the atop site is a poor representation of the true potential energy surface. Lie et al. studied vibrational properties of hydrogen on the Rh(111) surface using DFT methods.[4] They found that the potential energy surface is very anharmonic and there is a strong coupling between parallel and perpendicular motions due to the strong anharmonicity of the potential. Anderson et al. studied anharmonic properties of methoxy intermediate, adsorbed on a Cu(100) surface by surface infrared overtone spectroscopy and DFT electronic structure calculations.[5] In this investigation, the anharmonicity was measured in the zero-coverage limit, and it is observed that the anharmonicity is increased upon adsorption as compared with the free methanol. They demonstrated that modifications for anharmonicity of the methoxy species are indeed induced by adsorption onto the copper surface and not by the formation of

* To whom correspondence should be addressed. E-Mail: parsafar@sharif.edu.

10.1021/jp061576z CCC: $33.50
Published on Web 09/14/2006

the methoxy species. Kurten et al. calculated the one-dimensional potential energy profiles along the N−H and N−Ni bonds and vibrational wavenumbers of NH_3 adsorbed on the Ni(111) surface using DFT calculations.[6] They fitted one-dimensional potential energy profiles to an analytical expression using an accurate anharmonic potential model and concluded that when anharmonicity effects are taken into account, the vibrational frequencies are in good agreement with the experimental data.

Adsorption of CO on different Ni surfaces has been propounded in industry before. The most important industrial applications of the CO/Ni adsorption system are in methane reforming and Fischer−Tropsch synthesis.[7−9] Therefore, there are a considerable number of articles in which the electronic and geometrical structures of this system have been studied. Eichler[10] and Shah et al.[11] performed a comprehensive DFT calculation for CO adsorption on different Ni surfaces and especially for the Ni(111) surface. The later researchers used the calculated density of states, DOS, diagrams for CO adsorption on the Ni(111) surface before and after the adsorption, from which they suggested that 5σ and 2π molecular orbitals of CO have the strongest interactions with Ni surface atoms.[11] Both mentioned researchers have shown that the adsorption of CO on the hcp site of Ni(111) surface is the strongest. In these articles, the potential energy of adsorptive bond versus distance of the CO molecule from the surface is not reported. Xu et al. performed the complete active-space multiconfiguration self-consistent field, CASSCF, calculations for the ground states of Ni−CO and Fe−CO bonds and emphasized that a balance between σ/π interactions has a very important role in the stability of these types of bonds.[12]

In 1999, Elliott and Ward[13] developed a quantum statistical approach to study the adsorption of diatomic gases on single crystalline surfaces. They used an ideal model to calculate some thermodynamic properties of the adsorbed CO gas on a Ni(111) surface, including the chemical potentials. The adsorption of CO on a Ni(111) surface predominantly has only one type of adsorptive bond,[14] especially when the coverage is less than 0.5 ML in which the CO molecules are perpendicular to the surface and multibonded.[15] Quiroś et al. studied CO adsorption on a Ni(111) surface using X-ray diffraction in an ultrahigh vacuum (UHV) environment in a pressure range from 10^{-6} to 1.2 bar.[16] They indicated that, in this pressure range, ordered structures close to $\sqrt{7} \times \sqrt{7}R19.1°$ occur. In these circumstances, the coverage is more than 0.5 ML, and the side-by-side interactions are important in such a way that the intermolecular distance of adsorbed CO on Ni(111) depends on the CO pressure in the chamber and there is a reversible compression/expansion of adsorbed CO on a Ni(111) surface at room temperature. At atmospheric pressures, most of the molecules sit on low-symmetry sites. Quiroś et al. showed that the compressibility of the adlayer arises from a repulsive force between the CO molecules on the surface. Also, there is an abundance of experimental data for the geometry and thermodynamic properties, especially for the adsorption isotherms.[17−18] Because of these facts, the CO/Ni(111) adsorption system is an appropriate case for theoretical investigations. To obtain the vibrational partition function for the adsorbed CO molecule, Eillott and Ward used a harmonic oscillator model and assumed random distribution for the adsorbed CO molecules on the lattice sites. Using such an ideal model, they obtained the following expression for the canonical partition function (Q^σ) of the adsorbed molecules as:[13]

$$Q^\sigma = \frac{AM!}{N^\sigma!(AM - N^\sigma)!}(q_1, q_2, ..., q_6)^{N^\sigma} \tag{1}$$

$$q_i = \frac{\exp\left(-\frac{\epsilon'_{0,i}}{kT}\right)}{1 - \exp\left(-\frac{\hbar\omega_i}{kT}\right)} \tag{2}$$

$$\epsilon'_{0,i} = E'_0\frac{\omega_i}{\sum_{i=1}^{6}\omega_i} + \frac{\hbar\omega_i}{2} \tag{3}$$

where M is the number of sites per unit area, N^σ is the number of adsorbed molecules, A is the area of surface, and E'_0 is the potential energy of the adsorbed molecules, which is related to the intermolecular interactions of the adsorbed molecules, which of course, depends on the coverage, ω_i and q_i are the angular frequency and the corresponding partition function of the ith vibrational mode of adsorbed CO molecule, respectively, and k is the Boltzmann constant. They used the vibrational partition function to obtain the following expression for the chemical potential of the adsorbed molecules,[13], μ^σ, as:

$$\mu^\sigma(T, N^\sigma) = \left(\frac{\partial F^I}{\partial N^\sigma}\right)_{T,A} \tag{4}$$

$$\mu^\sigma(T, N^\sigma) = kT \ln\left[\frac{N^\sigma}{(AM - N^\sigma)\,\psi\,\exp\left(\frac{b - \beta'}{kT}\right)}\right] \tag{5}$$

where F^{I} is the Helmholtz free energy of the adsorbed molecules and

$$\psi(T) = \prod_{j=1}^{2}\frac{\exp\left(\frac{\hbar\omega_j}{2kT}\right)}{\exp\left(\frac{\hbar\omega_j}{kT}\right) - 1} \tag{6}$$

$$b(T) = kT \ln\left[\prod_{i=3}^{6}\frac{\exp\left(\frac{\hbar\omega_i}{2kT}\right)}{\exp\left(\frac{\hbar\omega_i}{kT}\right) - 1}\right] \tag{7}$$

$$\beta'(N^\sigma) = \frac{\mathrm{d}(E'_0N^\sigma)}{\mathrm{d}N^\sigma} \tag{8}$$

In the above expressions, six vibrational degrees of freedom of adsorbed CO on Ni(111) surface are divided into two categories: w_1 and w_2, which are known experimentally,[19] and w_3, ..., w_6, for which there are no experimental data. Therefore, they used experimental isotherms to obtain the values of $b(T)$ and $\beta'(N^\sigma)$ for temperatures for which experimental data are available. As mentioned, they assumed all vibrational modes to be harmonic. At least for the stretching mode of CO perpendicular to the surface, such an assumption seems to be unrealistic because of the fact that the media on two sides of the vibration are quite different: one medium is hard (surface) and the other is soft (gas).

In this work, first, we have used the density functional theory (DFT) to calculate the effective potential function for the

adsorption of the CO molecule on the Ni(111) surface, which is expected to be quite anharmonic. Using these potential surfaces, we calculated those vibrational frequencies for which experimental data exist and investigate harmonic and anharmonic shift of these frequencies. Second, two model potentials are used for the adsorptive bond to obtain the canonical partition function of the adsorbed species in such a way that their Schrödinger equation can be solved analytically and, therefore, we can obtain an analytical expression for the partition function. These potential models are, namely, the soft attraction−hard repulsion (HS) and Morse potential (MP) models. The HS model does not completely correspond to the physical reality of the system but can be used to compare its properties with other potential models in order to indicate effect of the model potential on the thermodynamic properties of adsorptive bond. The calculated partition function is used to calculate thermodynamic properties for both models. The importance of the chosen model potentials on the thermodynamic properties of the adsorptive bond is investigated.

Calculation of Adsorption Potential

To calculate the partition function of the adsorbed CO molecule on the Ni(111) surface, the interaction potential energy between the surface and adsorbed molecule as a function of distance is needed. To do such a task, the potential function is calculated using the Vienna ab initio simulation package (VASP), which solves self-consistently the Kohn−Sham equations[20] by developing the electronic wave functions in a plane wave basis set. The generalized gradient approximation (GGA), using the functional of Perdew and Wang[21] (PW91), is employed. As shown in the previous calculations, this functional gives reasonable results for many transition metals.[22−26] The electronic wave functions were expanded as linear combinations of plane waves, truncated to include only plane waves with kinetic energies below a prescribed cutoff energy, 400 eV. Because of the delocalized nature of the itinerant electrons within the lattice, a delocalized, plane-wave basis set provides a good representation of metallic systems. The core electrons are replaced by pseudopotentials to render the computations tractable as well as to enhance efficiency.[27] The *k*-space sampling was performed using the Γ-centered grid[28] because we found that the energy converges significantly faster with the Γ-centered grid than with the standard Monkhorst−Pack[29] grid in this work. A *k*-point mesh of $4 \times 4 \times 1$ is employed for the relaxation calculations and a $6 \times 6 \times 1$ grid for the potential energy calculations. The pseudopotentials for Ni, C, and O, which are given in the VASP package, are used for all calculations. The Ni(111) surface is modeled using the supercell approach, where a periodic boundary condition is applied to the central supercell so that it is reproduced periodically throughout the space. The surface is cleaved from a faced-centered cubic (fcc) crystal structure of Ni, corresponding to the (111) Miller plane, which comprised five Ni layers. The surface is produced by replication of the central supercell in the *x*−*y* plane, as shown in Figure 1. A vacuum spacing of 16 Å is considered in the *z* direction to prevent any interaction between the mirror images. An optimized lattice constant value of 3.532 Å is obtained by the bulk cell optimization using the same computational parameters. To model the adsorption, a CO molecule is adsorbed on any possible site of the first layer of the slab and the three topmost layers are allowed to relax while two bottom layers are fixed. The CO adsorption is considered as a monolayer coverage (ML) of 0.25, corresponding to the p(2 × 2) arrangement for the on-top, bridge, fcc, and hcp sites, as shown in Figure 2a, b, c, and d, respectively. Note that, in these figures, only two topmost layers of the Ni(111) surface are shown in order to avoid any complexity in representing various adsorption sites of the Ni(111) surface. The results for geometry optimizations are compared with those of Eichler[10] and Shah et al.[11] in Table 1.

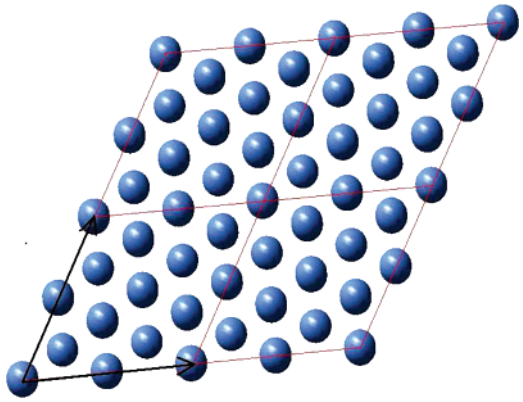

Figure 1. Replication of supercell in *x*−*y* plane such that the periodic boundary condition of the slab model is included.

TABLE 1: Results Obtained from Geometry Optimizations Compared with Those of Eicchler[10], Shah et al.[11] in $\theta = 0.25$ ML, and This Work for CO Adsorption on Ni(111) Surface, Where d_{C-O} Is C−O Bond Distance, d_{C-Ni} Is the Bond Length between C and the nearest Ni Atom, and Z_C Is the Distance of CO Molecule from the Surface

sites	d_{C-O} (Å)	d_{C-Ni} (Å)	Z_C (Å)	E_{ads} (eV)[d]
on-top	1.161[a]	1.75[b]	1.837[a]	1.55[a]
	1.161[c]	1.74[c]	1.740[c]	1.55[b]
bridge	1.183[a]	1.88[b]	1.439[a]	1.80[a]
	1.181[c]	1.882[c]	1.404[c]	1.78[b]
fcc	1.191[a]	1.95[b]	1.337[a]	1.90[a]
	1.190[c]	1.953[c]	1.343[c]	1.87[b]
hcp	1.192[a]	1.95[b]	1.321[a]	1.93[a]
	1.191[b]	1.955[c]	1.338[c]	1.90[b]

[a] Data of Eichler.[10] [b] Data of Shah et al.[11] [c] Data of this work. [d] $E_{ads} = E_{CO} + E_{slab} - E_{CO/slab}$.

Now, to obtain the potential function of the adsorptive bond, we might change statically the CO−surface distance, *r*, step by step. The calculated interaction energy (*E*) versus the distance *r* is plotted in Figure 3. It is clear that the potential function for the adsorptive bond is significantly different from a harmonic oscillator model used by Elliott and Ward, i.e., the anharmonicity contribution of the adsorptive bond is significant.

There are many calculated results in the literature for the CO−Ni bond of the $Ni(CO)_n$ complexes. Doerr et al. calculated dissociation energy D_0 for the CO−Ni bond to be 27 kcal/mol by using the DFT method for the $Ni(CO)_4$ complex.[30] Petz et al. calculated D_0 for the CO−Ni bond to be 16.3 kcal/mol by using the DFT with the B3LYP hybrid functional for some Ni complexes with CO and C(PPh3) ligands.[31] Our calculations predict values of 151, 178, 192, and 196 kJ/mol for the potential well depth, D_e, for the on-top, bridge, fcc, and hcp sites, respectively, compared to 170 ± 24 kJ/mol of the experimental data for the D_0 of the Ni−CO particle.[32] Our calculated value of D_e for the CO−Ni adsorptive bond is reasonable due to the fact that an adsorptive bond is to some extent different from the corresponding bond in a molecule because of the different local interactions on the lattice sites. Because CO molecules are adsorbed perpendicularly and multibonded on the Ni(111) surface when coverage ≤ 0.5[15] and the hcp site is the most suitable one, we may assume that the adsorption is mainly taking place on this site.

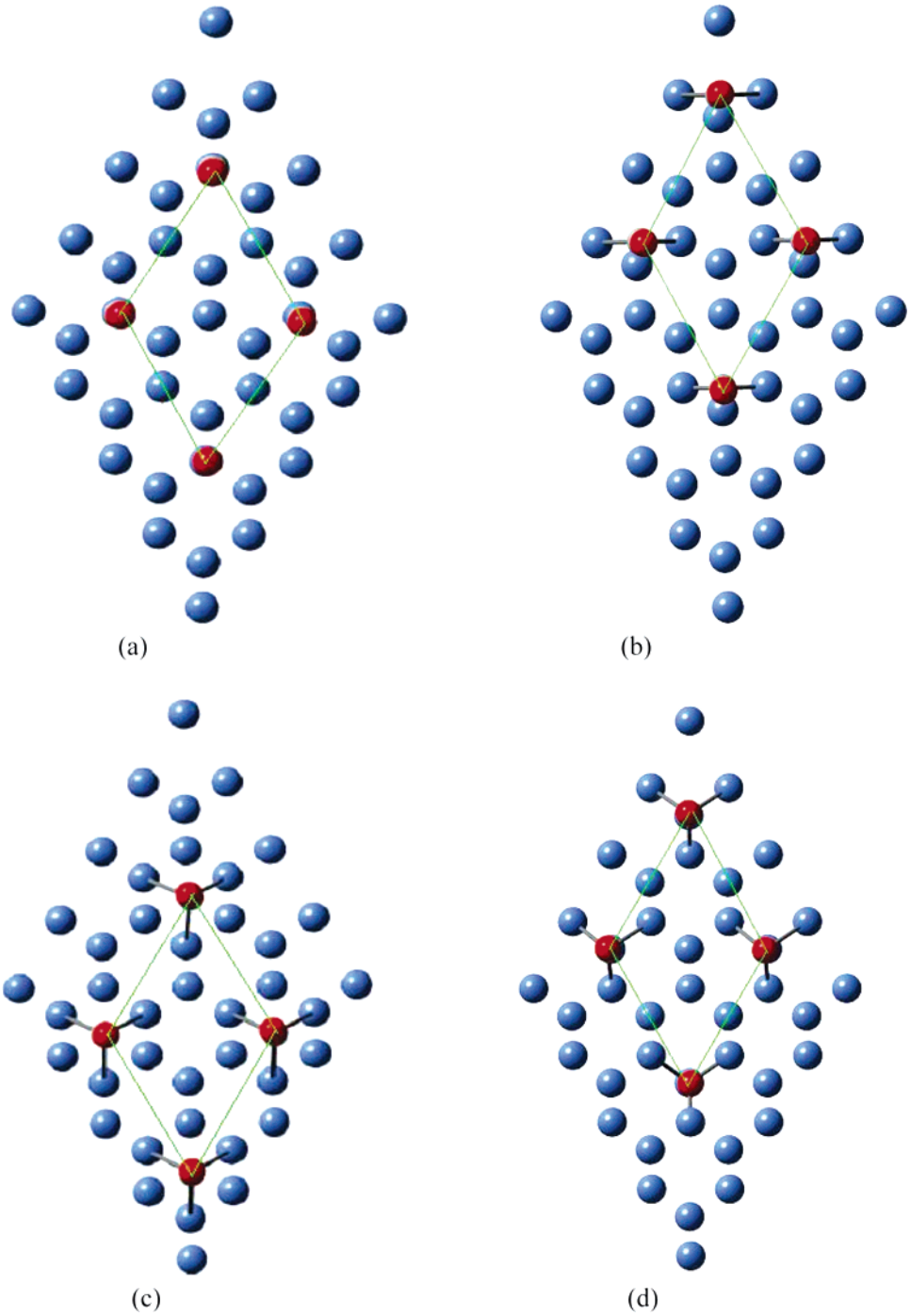

Figure 2. p(2 × 2) arrangement of adsorbed CO molecules on Ni(111) surface that are used in the relaxation calculations. The adsorption on the on-top, bridge, fcc, and hcp sites are shown in (a), (b), (c), and (d), respectively.

After the calculation of adsorption potential, the harmonic and anharmonic frequencies of the C−surface and C−O bonds for the hcp site were calculated. The harmonic frequency of each bond was obtained by fitting five points around the minimum point of adsorption potential in a quadratic function. The anharmonic frequencies were calculated by fitting the same points in a Morse potential function:[33]

$$U(x) = D_e(1 - \exp(-\beta x))^2, \qquad \upsilon = \beta\left(\frac{D_e}{2\pi^2\mu}\right)^{1/2} \quad (9)$$

where D_e is the potential well depth and υ and μ are the anharmonic frequency and reduced mass, respectively. The results for the harmonic and anharmonic shifts of calculated frequencies are compared to experimental data in Table 2. As shown in Table 2, the anharmonicity effect of the adsorptive bond is considerably more than that of the C−O bond. Because the stretching frequencies of the C−surface and C−O bonds are far from each other and the interaction between CO and the Ni(111) surface is very weak compared to the strength of the C−O bond, the mixing of the CO internal mode with the C−surface mode is negligible[34,35] and we may discard the anharmonic coupling between these vibrational modes. This behavior is also observable in $Ni(CO)_n$ complexes.[36] An example is the $Ni(CO)_4$ complex, in which the C−O stretching frequency is 1994.5 cm^{-1} but the Ni−C stretching frequency is 591.1 cm^{-1}.

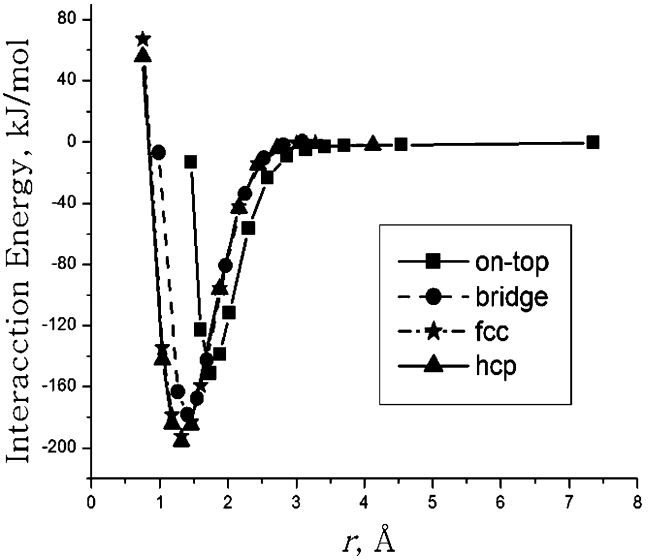

Figure 3. The calculated interaction energy of adsorbed molecule vs distance of CO from the surface, *r*, for four different adsorption sites.

Hence, we have calculated thermodynamic properties of the adsorptive bond by assuming that the adsorption occurred on the hcp site only. Our calculated D_e is the energy difference of the adsorptive bond between the equilibrium distance and a distance far from the surface (up to 8 Å), and it is a little different from the adsorption energy calculated by Eichler[10] and Shah et al.[11] This difference is due to the fact that, in scanning the CO distance from the surface to find D_e, we do not change the CO internal bond distance and fix it at its equilibrium distance in the adsorbed form because we have assumed that the vibrational modes of CO on the surface are independent, whereas in the calculated adsorption energies by Eichler and Shah et al., the CO bond distance in E_{co} was set to be the gas-phase value. We may note that the calculated value for D_e is larger than that of the actual value. The additional value is equal to the energy difference between the adsorbed CO and the CO that is 8 Å apart from the surface; therefore, we have calculated this difference for the hcp site and subtracted this value from the previously calculated D_e. The difference is found to be 11 kJ/mol.

Because we wish to have an analytical expression for the energy levels, we may propose some model potentials for which the Schrödinger equation can be solved analytically and used to calculate the partition function and thermodynamic properties.

Calculation of Thermodynamic Properties Using the HS Model. A HS potential model may be represented as:

$$u(x) = \begin{cases} \infty & x < x_e \\ ax^2 & x \geq x_e \end{cases} \tag{10}$$

where x_e is the equilibrium bond length. Solution of the Schrödinger equation for this model is simple and similar to that for the harmonic oscillator, whereas in this case, only those wave functions that pass through the origin are acceptable. Therefore, the wave functions of the harmonic oscillator with odd quantum numbers are acceptable for such a model. Considering such a constraint for the harmonic oscillator wave functions, we may obtain a simple relation for the quantum mechanical energy levels of the HS model as:[37]

$$E_n = h\nu(2n + {}^3/_2), \qquad n = 0, 1, 2, ... \tag{11}$$

where h is the Planck constant and ν is the classical vibration frequency. Note that, like the harmonic oscillator potential function, the attraction wall of the HS model is a quadratic function; however, the repulsion wall is hard, like that of the hard sphere model.

We may use eq 11 to derive the partition function as:

$$Q^\sigma = \frac{AM!}{N^\sigma!(AM - N^\sigma)!}(q'_{HS,1}, q_2, ..., q_6)^{N^\sigma} \tag{12}$$

when

$$q_{HS} = \frac{\exp\left(-\frac{3\theta_v}{2T}\right)}{1 - \exp\left(-\frac{2\theta_v}{T}\right)} \tag{13}$$

$$q'_{HS,1} = \exp\left(-\frac{x_1 E'_0}{kT}\right) q_{HS,1} \tag{14}$$

$$E'_0 = \sum_{i=1}^{6} x_i E'_0 \tag{15}$$

where the contribution of each vibrational degree of freedom in E'_0 is taken as an unknown value, x_i, where $0 < x_i < 1$ and $\sum_{i=1}^{6} x_i = 1$, and it does not appear in the thermodynamic properties. We may calculate the chemical potential for the adsorbed molecules using the thermodynamic characteristic function of the canonical ensemble, eq 4. The result is the same as eq 5, except that the expression for $\psi(T)$ given in eq 6 is replaced by $\psi'(T)$ as:

$$\psi'(T) = \left(\frac{\exp\left(\frac{\hbar\omega_1}{2kT}\right)}{\exp\left(\frac{2\hbar\omega_1}{kT}\right) - 1}\right) \cdot \left(\frac{\exp\left(\frac{\hbar\omega_2}{2kT}\right)}{\exp\left(\frac{\hbar\omega_2}{kT}\right) - 1}\right) \tag{16}$$

where ω_1 is the angular frequency for the adsorptive bond and ω_2 for the internal CO stretching mode. The obtained expression for the adsorption isotherm is the same as that given by Elliott and Ward, with the exception that $\psi(T)$must be replaced by $\psi'(T)$, i.e.,

$$P_e(T, \theta_e) = \frac{\theta_e}{(\theta_M - \theta_e)\psi'\varphi \exp\left(\frac{b - \beta'}{kT}\right)} \tag{17}$$

where $P_e(T, \theta_e)$ is the pressure of the gas phase at equilibrium with the adsorbed phase, and:

TABLE 2: Harmonic (ν_h) and Anharmonic (ν_{an}) Frequencies of C−surface and C−O Stretching Modes Calculated with DFT Compared to Experimental Data (ν_{exp}) for the Adsorption of CO on the hcp Site of Ni(111) Surface

bond	ν_{exp}[19] (cm^{-1})	ν_h (cm^{-1})	ν_{an} (cm^{-1})	$\Delta(\nu_h - \nu_{exp})$ (cm^{-1})	$\Delta(\nu_{an} - \nu_{exp})$ (cm^{-1})	$\Delta(\nu_h - \nu_{an})$ (cm^{-1})
C−surface	410.1	377.1	387.5	−33	−22.6	−10.4
C−O	1856.8	1866.5	1864.6	9.7	7.8	1.9

$$\theta_M = \frac{M}{M_0}, \qquad \theta_e = \frac{N^\sigma}{AM_0} \tag{18}$$

Because CO molecules adsorb perpendicularly and multibonded on the Ni(111) surface when the $\theta_e \leq 0.5$,[15] we have used the experimental Christmann isotherms for all for which θ_e is less than 0.5 ML. We have used the method of Elliott and Ward to calculate the adsorption isotherms. The average deviations of calculated pressures from experimental data for H, HS, and MP models have been shown in Figure 4a. The average overall deviation in pressure from experimental data is found to be 1.4% for HS and 5.8% for MP, compared to 6.1% for the H model. Hence, the HS model gives better results for adsorption isotherms in comparison with H and MP models. These results indicate that, if anharmonicity of adsorptive bond is taken into account, the overall deviation of calculated pressure from the experimental value becomes less. Although including anharmonicity leads to better results for adsorption isotherms, the differences between mentioned models are not significant. The mean differences of calculated pressures for Christmann isotherms given by the H, HS, and MP models versus T are shown in Figure 4b. As shown in this figure, as temperature increases, in which the anharmonicity becomes significant, the differences between the calculated pressures are more noticeable.

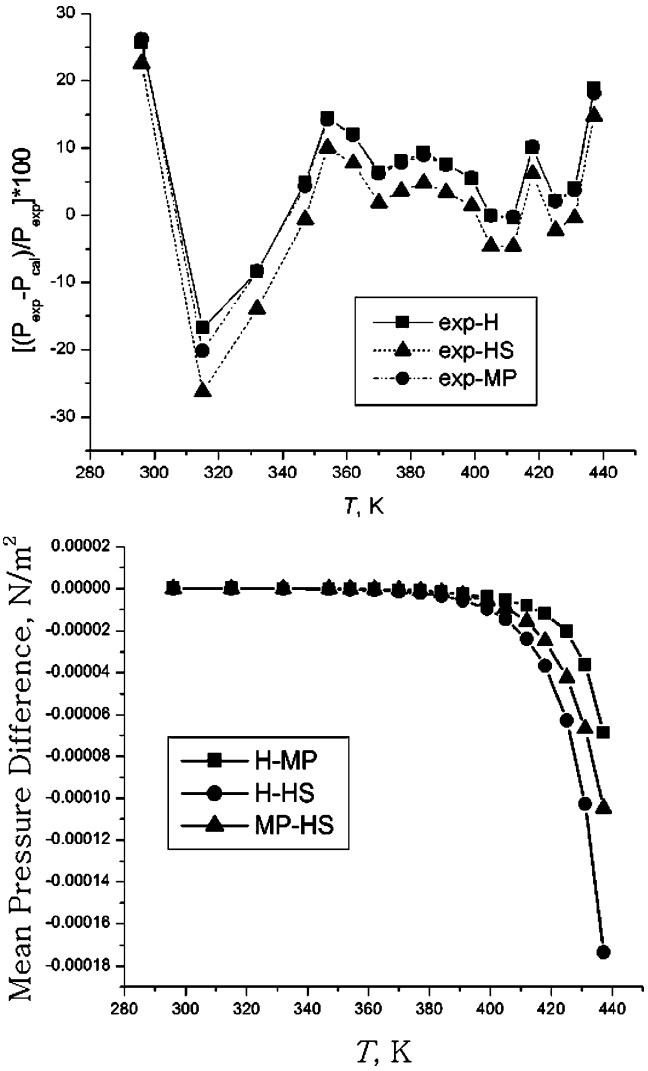

Figure 4. Mean deviations of the calculated pressures from experimental isotherms, obtained from the HS, MP, and H models versus temperature (a). Mean differences of the calculated pressures from each other, obtained from the HS, MP, and H models vs temperature (b).

Three important thermodynamic properties, namely the internal energy, E, isochoric heat capacity, C_v, and entropy, S, are calculated using the HS model. The internal energy, heat capacity, and entropy may be given as follows:[38]

$$E = NkT^2\left(\frac{\mathrm{d} \ln q_{\mathrm{vib}}}{\mathrm{dT}}\right) \tag{19}$$

$$C_v = \left(\frac{\partial E}{\partial T}\right)_{N,V} \tag{20}$$

$$S = Nk \ln q + \frac{E}{T} + C \tag{21}$$

Equations 19 and 20 may be used to obtain E and C_v for the HS model as

$$E_{\mathrm{HS}} = Nk\left(\frac{3\theta_v}{2} + \frac{2\theta_v}{\exp\left(\frac{2\theta_v}{T}\right) - 1}\right) \tag{22}$$

$$C_{v,\mathrm{HS}} = Nk\left(\frac{2\theta_v}{T}\right)^2 \frac{\exp\left(\frac{2\theta_v}{T}\right)}{\left(\exp\left(\frac{2\theta_v}{T}\right) - 1\right)^2} \tag{23}$$

The calculated results for E, C_v, and S versus T for the HS and H models are shown in Figures 5, 6, and 7, respectively.

Calculation of Thermodynamic Properties Using the MP Model. The oscillatory energy levels for the Morse potential are given by:[33]

$$E_n = h\nu[(n + {}^1/_2) - x_e(n + {}^1/_2)^2 + y_e(n + {}^1/_2)^3 - ...], \quad n = 0, 1, 2, ... \tag{24}$$

in which x_e, y_e, ... are anharmonicity constants. Because of the infinite number of terms in eq 24, one is not able to calculate an analytical expression for the partition function. However, because x_e is significantly larger than other inharmonicity coefficients,[33] we may truncate the terms after the quadratic one in eq 24. Because when a molecule is far enough from the surface, it will not belong to the adsorption phase any more, we may assume that a molecule belongs to the adsorption phase if its energy does not exceed D_e. Hence, we may assume that the upper limit of vibrational energy level for an adsorptive bond is D_e.

We may use such an upper bond limitation for the energy levels along with the truncated eq 24 to obtain the highest energy level, $n_{\max}$, corresponds to D_e as:[33]

$$n_{\max} = \frac{1}{2x_e} - \frac{1}{2} \tag{25}$$

where

$$D_e = \frac{h\nu}{4x_e} \tag{26}$$

For the adsorption of CO on the Ni(111) surface, with D_e = 185 kJ/mol $\omega = 7.73 \times 10^{13}$ s^{-1}, we obtain $x_e = 0.006\,649$ and $n_{\max} = 74$.

Using the truncated eq 24, we may obtain the canonical partition function of the MP model (q_{MP}) for the adsorption bond as:

$$q_{\mathrm{MP}} = \sum_{n=0}^{n_{\max}} \exp\left(-\frac{\theta_v}{T}[(n + {}^1/_2) - x_e(n + {}^1/_2)^2]\right) \tag{27}$$

Because the partition function for the other degrees of freedom are assumed to be harmonic, the total partition function for the adsorption phase may be written as:

$$Q^{\sigma} = \frac{AM!}{N^{\sigma}!(AM - N^{\sigma})!}(q'_{\mathrm{MP}}, q_2, ..., q_6)^{N^{\sigma}} \tag{28}$$

$$q'_{\mathrm{MP}} = \exp\left(-\frac{x_1 E'_0}{kT}\right) q_{\mathrm{MP}} \tag{29}$$

$$q_i = \frac{\exp\left(-\frac{\left(x_i E'_0 + \frac{\hbar\omega_i}{2}\right)}{kT}\right)}{1 - \exp\left(\frac{\hbar\omega_i}{kT}\right)}, \qquad i = 2, ..., 6 \tag{30}$$

$$E'_0 = \sum_{i=1}^{6} x_i E'_0 \tag{31}$$

where the contribution of each vibrational degree of freedom in E'_0 is taken as an unknown value x_i, where $0 < x_i < 1$.

By having the total partition function, the chemical potential of adsorbed molecules may be calculated from eq 4 as:

$$\mu^{\sigma}(T, N^{\sigma}) = kT \ln\left[\frac{N^{\sigma}}{(AM - N^{\sigma})\,\psi' \exp\left(\frac{b - \beta'}{kT}\right)}\right] \tag{32}$$

Note that the obtained expression for μ is the same as that given by eq 5, except that ψ is replaced by ψ'', where

$$\psi''(T) = q_{\mathrm{MP}}\left(\frac{\exp\left(\frac{\hbar\omega_2}{2kT}\right)}{\exp\left(\frac{\hbar\omega_2}{kT}\right) - 1}\right) \tag{33}$$

Also, the expression for the adsorption isotherm is the same as eq 16, except that ψ' is replaced by ψ''.

Also, the deviation of pressures calculated by the MP model from the experimental data have been shown in Figure 4a, and differences between MP pressures and the other models are shown in Figure 4b. The expressions for the thermodynamic properties, E, C_v, and S, may be obtained for the MP model as

$$E_{\mathrm{MP}} = Nk\theta_v \times \left(\frac{\sum_{n=0}^{n_{\max}} ((n + {}^1/_2) - x_e(n + {}^1/_2)^2) \exp\left(-\frac{\theta_v}{T}((n + {}^1/_2) - x_e(n + {}^1/_2)^2)\right)}{q_{\mathrm{MP}}}\right) \tag{34}$$

$$C_{v,\mathrm{MP}} = Nk\left(\frac{\theta_v}{T}\right)^2 \times \left(\frac{\sum_{n=0}^{n_{\max}} (((n + {}^1/_2) - x_e(n + {}^1/_2)^2))^2 \exp\left(-\frac{\theta_v}{T}((n + {}^1/_2) - x_e(n + {}^1/_2)^2)\right)}{q_{\mathrm{MP}}}\right) - Nk\left(\frac{\theta_v}{T}\right)^2 \left(\frac{\left(\sum_{n=0}^{n_{\max}} ((n + {}^1/_2) - x_e(n + {}^1/_2)^2) \exp\left(-\frac{\theta_v}{T}((n + {}^1/_2) - x_e(n + {}^1/_2)^2)\right)\right)^2}{{q_{\mathrm{MP}}}^2}\right) \tag{35}$$

The expression for S is the same as that of eq 21, except that q must be replaced with q_{MP}. The calculated results for E, C_v, and S versus T for both the MP and HS models are shown in Figures 5, 6, and 7, respectively. Also, the calculated entropies versus the internal energy and partition functions versus temperature obtained from different potential models are plotted as shown in Figures 8 and 9, respectively.

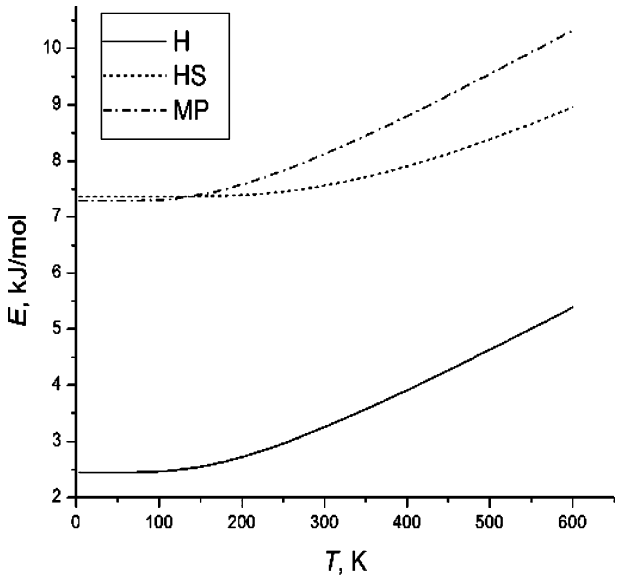

Figure 5. Calculated internal energy for the adsorptive bond vs temperature, using the H, HS, and MP models. Note that the zero-point energy of H is quite different from that of two other models, and the trend of energy with respect to temperature are comparable for all models.

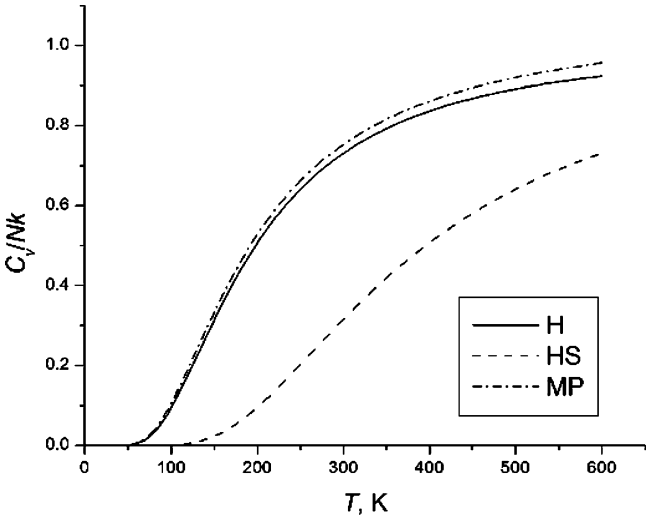

Figure 6. Same as Figure 5 for the isochoric heat capacity.

Discussion

The calculated D_e for various types of CO adsorption are reasonable, although we used DFT methods to calculate the potential energy of CO adsorption on each type of adsorption sites. For small molecules and systems with a limited number of electrons, usually DFT methods do not give exact results for interaction energies. However, in this work, the results for potential well, D_e, seem to be reasonable in comparison with experimental data for complexes containing the Ni−CO bond. The reasons for this reasonableness are not exactly clear due to the fact that the DFT methods are based on the Kohn−Sham equations and the solution to them gives the Kohn−Sham

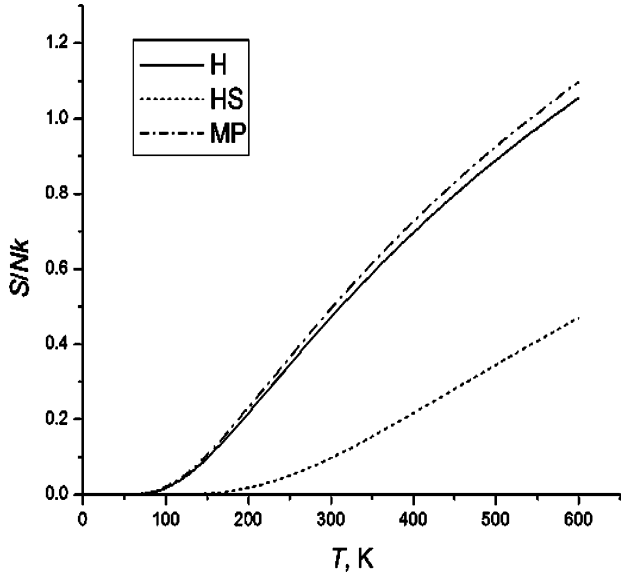

Figure 7. Same as Figure 5 for entropy.

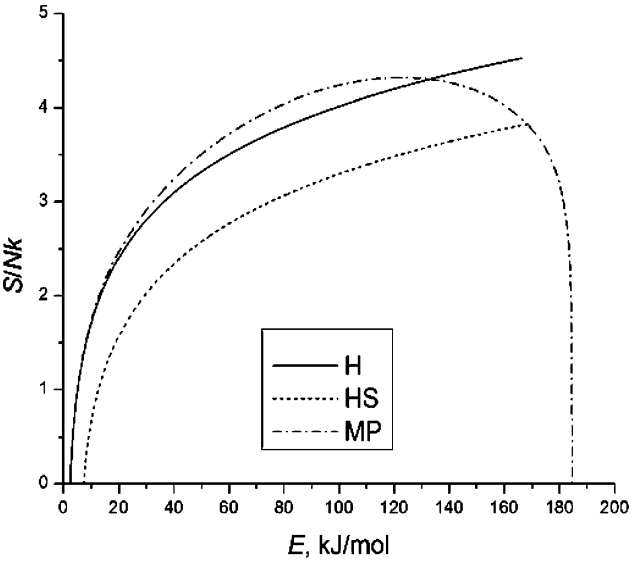

Figure 8. Calculated entropy for the adsorptive bond vs internal energy, using the H, HS, and MP models.

orbitals that do not have any physical interpretation and only are used to obtain the ground-state energy of the system. However, we may give such reasonableness of D_e as follows: First, there are many free electrons in metallic systems, thus the initial guess in solving Kohn−Sham equations using DFT calculations in which many electron systems are considered as a uniform electronic gas in local density approximation, LDA, seems to be reasonable. Second, in the slab model, the periodic boundary condition is included; therefore, the environment around an atom in the surface is mainly similar to that of the real case.

Because we have investigated the adsorption for the cases that $\theta < 0.5$ ML, the side-by-side interactions among the adsorbed molecules may be discarded. This is due to the fact that, on the basis of Quiroś et al. investigation, the side-by-side interactions among the CO molecules are repulsive, therefore, CO molecules on the surface tend to be farther from each other than we may expect that at low coverage, and the environment around each adsorbed molecule is similar to that of the others. In other words, at low coverage, potential energy due to the side-by-side interactions is the same for all adsorbed molecules

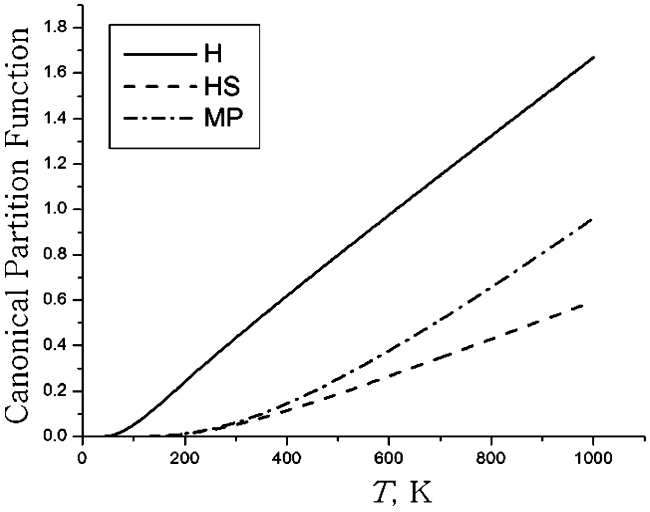

Figure 9. Calculated partition function for the adsorptive bond vs temperature using the H, HS, and MP models.

and may be considered as an additive constant to total energy and does not affect thermodynamic properties. However, as reported by Quiroś et al., when $\theta > 0.5$ ML, the side-by-side interactions become significant. Thus, at high coverage, the side-by-side interactions should be taken into account.

Because of the fact that, at low temperatures, most of the molecules are in the vibrational ground state, which vibrate within their equilibrium positions, the harmonic model is reasonable for internal molecular vibrations. Also, the shape of the potential function of the oscillator is similar to the harmonic one about the equilibrium distance. As shown in Table 2, the vibrational frequency of the internal CO bond on the Ni(111) surface is larger than that of the adsorptive bond by a factor of more than four, we may discard the coupling of these degrees of freedom. Moreover, the anharmonicity effect of the adsorptive bond is much greater than that of C−O bond, the anharmonicity of C−O may be ignored. Because the adsorbed CO molecule on the Ni(111) surface has a stretching vibrational mode perpendicular to the surface for which the mode is faced with two different mediums (solid and vacuum), such a vibration is expected to deviate from a harmonic oscillator significantly. Therefore, for the reason given above, we have discarded the anharmonicity for the CO bond. We used a DFT calculation to obtain the interaction potential for such a mode. The calculated potential can be fitted on the MP model because of the fact that this model is consistent with the physical reality of the system, but this is not the case for HS model because of the fact that, even though its repulsive wall is considered as a limit of the real repulsion wall, its attraction wall does not reflect any physical reality of the system.

On the basis of results shown in Figure 4a and b, we have calculated pressure that is not considerably very sensitive to the model potentials in such a way that the average deviation from the experimental data are less than 8% (see Figure 4a). The reason for such insensitivity may be due to the existence of two adjustable parameters, $b(T)$ and $\beta'(\theta)$, whose values are obtained by using the experimental data. However, if side-by-side interactions and all types of adsorption sites are taken into account, we may expect that the calculated pressures would be in better agreement with experimental data. On the basis of the results shown in Figure 4b, the calculated pressures obtained from the MP and HS models are more than that of the H model, indicating that the pressure of the gas phase in equilibrium with the adsorption phase for MP and HS models are more than that of the H model. Because the chemical potential varies mono-

tonically with pressure, and at equilibrium, the chemical potential of the adsorption and gaseous phases are equal, therefore, MP and HS models predict the chemical potential of the adsorption phase more than that of the harmonic model. In other words, two former models predict a more unstable phase for the adsorbed system thermodynamically. On the basis of Figure 9, the calculative partition function of adsorptive bond using the H model is more than those of the MP and HS models, and the partition function of the adsorptive bond calculated from the MP model is more than that of the HS model. Because all of the partition functions of the adsorptive bond in the temperature range of the Christmann isotherms are less than one, their logarithm will be negative and hence a larger value of the partition function will give a smaller value for the chemical potential, i.e., the H model gives the most stable adsorption phase again (Note that, for the canonical ensemble, $\mu = -kT \ln(q/N)$). Also, it may be noted that, in the range of experimental isotherms, the temperature is low enough that the higher energy levels are not significantly important, and partition function which is a measure for the availability of the energy levels for the H model is more than those for the MP and HS models. However, at higher temperatures, the differences in the partition functions of the various potential models become more significant due to the fact that, at higher temperatures, higher energy levels involve more and distribution of the adsorbed particles on energy levels depends on the spacing between energy levels, and we may expect that the differences become more significant. See the trend of the calculated pressure differences in Figure 4b. Because of the fact that the anharmonicity effects become more significant at high temperatures, larger differences in the calculated pressures are expected.

As shown in Figure 5, the trend of the calculated energy given by different models is insensitive to the models at low temperatures. However, unlike the other models, because the MP model has an upper energy level ($n_{max} = 74$), the difference between the calculated energy given by the MP is significant with that of the other models at high temperatures. Note that the MP model has a maximum energy of NE_{max} at very high temperatures, which are not shown in Figure 5, but the other models have no upper bond energy where E_{max} is the highest energy level. Note that the internal energy trend does not significantly depend on the spacing between energy levels due to the fact that the internal energy is the partial derivative of the partition function with respect to temperature and variation of temperature does not change the spacing between the levels. The calculated internal energy depends on the zero-point energy as well as the molecular populations on the energy levels, which later vary with temperature.

The calculated values of C_v are shown in Figure 6. As shown in this figure, the values given by the HS and H models are generally very small except at low and moderate temperatures. Note that, because the energy spacing for the energy levels for the H model is less than that of the HS, the former model gives a higher value of C_v. Both models would give the classical value of $C_v/Nk = 1$ when T approaches infinity. However, the value given by MP is quite different from those of the two other models. Because the energy spacing between the energy levels of the MP is less than that of two other models, the values of C_v given by the MP model is significantly larger than those of two other models at low and moderate temperatures. At higher temperatures, the molecular population on the highest energy level, n_{max}, becomes significant, and the value of C_v given by the MP declines with temperature. Such a behavior is expected because of the fact that such molecules on the $n_{max} = 74$ level cannot absorb heat any more. Unlike the H and HS models, the value of C_v given by the MP approaches zero at very high temperatures because, when energy of the vibration is equal to $\sum_{i=1}^{n_{max}} (N/n_{max}) E_i$, ($i = 1, ..., n_{max}$), there is a uniform molecular distribution on the energy levels corresponding to $T = \infty$ when the internal energy becomes equal to NE_{max}, and no more energy absorption will be allowed; therefore $C_v = 0$. As shown in Figure 6, the maximum difference of C_v between HS and H models and between MP and H models are about 69% and 3.5%, respectively. Because the heat capacity is more sensitive to the spacing between the energy levels in comparison with internal energy, effect of the model potential on the isochoric heat capacity is more significant.

The calculated entropies given by the three models are shown in Figure 7. Separation of the energy levels plays an important role in the value of the entropy. For this reason, the MP model with the least separation gives the highest values and the HS model with the most separation gives the lowest value for S at low temperatures. However, at very high temperatures at which the number of available energy levels has a significant effect on the number of distribution on the energy levels and hence on S, for the H and HS models (with infinite number of energy levels), S approaches infinity when T tends to infinity. However, for the MP model,

$$S = k \ln\left(\frac{N!}{\left[\left(\frac{N}{n_{max}}\right)!\right]^{n_{max}+1}}\right) \text{ or}$$

$$\frac{S}{Nk} = \ln(n_{max} + 1) = \ln 80 = 4.382$$

when T tends to infinity. If such a vibrational model has energy more than $E_{max} = (N/n_{max}) \sum_{i=0}^{n_{max}} \epsilon_i$, then population inversion occurs, hence the entropy decreases with energy increment: $(\partial S/\partial E)_v < 0$ because $(\partial S/\partial E)_{v,N} = 1/T$, which means that the absolute temperature becomes negative.[39−41] Such unusual behavior is expected for any system with a limited number of energy levels. To show how the absolute negative temperature occurs, the calculated entropies versus energy are shown in Figure 8. As shown in this figure, for $E > (N/n_{max}) \sum_{i=0}^{n_{max}} \epsilon_i$, the calculated entropy from the MP model decreases with E, which means that $T < 0$. Because the entropy is too sensitive to the spacing between energy levels, the effect of the model potential on the entropy of the adsorptive bond is significant. Such differences are not obvious in the graph of S as a function of T because its maximum at finite positive temperatures (at which the adsorption system does not exist physically) is not shown in Figure 7; however, it can be seen readily in Figure 8. As shown in Figure 7, the maximum difference of S between the HS and H models and between the MP and H models are about 55% and 4%, respectively. Also, the entropy may be affected by the side-by-side interactions in which the repulsive interactions between adsorbed molecules keep them away from each other. Therefore, one may expect that molecules do not distribute on the sites randomly, from which we may conclude that the configurational entropy decreases with the coverage.

Our overall conclusion is that the model potential and hence the anharmonicity for adsorptive bond does not significantly affect those thermodynamic properties which are not sensitive to the spacing between the energy levels such as adsorption isotherms, but its effect on those which are sensitive to the spacing between energy levels, such as heat capacity and entropy, is important. The differences may be small at very low temperatures, however, it becomes significant at high temper-

atures, even at room temperature (see Figures 6 and 7). Because of the fact that the anharmonicity effects become important at high temperatures, such a behavior is expected.

Acknowledgment. We thank Sharif University of Technology Research Council for financial support.

References and Notes

(1) McQuarrie, D. A.; *Statistical Mechanics*; Harper Collins Publishers: New York, 1976.
(2) Loffreda, D.; Delbecq, F.; Simon, D.; Sautet P. *J. Phys. Chem. B* **2001**, *105*, 3027.
(3) Titmuss, S.; Johnson, K.; King, D. A. *J. Chem. Phys.* **2002**, *16*, 8097.
(4) Lie, W.; Xie, D. *Surf. Sci*. **2004**, *550*, 15.
(5) Anderson, M. P.; Blomquist, J.; Uvdal, P. *J. Chem. Phys.* **2005**, *123*, 224714.
(6) Kurten, T.; Biczysko, M.; Rajamaki, T.; Laasonen, K.; Halonen, L. *J. Phys. Chem. B* **2005**, *109*, 8960.
(7) Liu, Z. W.; Jun, K. W.; Roh, H. S.; Park, S.-E. *J. Power Sources* **2002**, *111*, 283.
(8) Prabhu, A. K.; Radhakrishnan, R.; Oyama, S. Ted. *Appl. Catal., A* **1999**, *183*, 241.
(9) Klinke, D. J., II; Broadbelt, L. J. *Chem. Eng. Sci*. **1999**, *54*, 3379.
(10) Eichler, A. *Surf. Sci*. **2003**, *526*, 332.
(11) Shah, V.; Li, Tao.; Baumert, K. L.; Cheng, H.; Sholl, D. S. *Surf. Sci.* **2003,** *537*, 217.
(12) Xu, X.; Lu, X.; Wang, N. Q.; Zhang, Q. N.; Ehara, M.; Nakatsuji, H. *Int. J. Quantum Chem.* **1999**, *72*, 221
(13) Elliott, J. A. W.; Ward, C. A. *Langmuir*, **1997**, *13*, 951.
(14) Surnev, L.; Xu, Z.; Yates, J. T., Jr. *Surf. Sci.* **1988**, *201*, 14.
(15) Netzer, F. P.; Madey, T. E. *J. Chem. Phys*. **1982**,*76*, 710.
(16) Quiroś, C.; Robach, O.; Isren, H.; Orgejón, P.; Ferrer, S. *Surf. Sci*. **2003**, *522*, 161.
(17) Christmann, K.; Schober, O.; Ertl, G. *J. Chem. Phys*. **1974**, *60*, 4719.
(18) Gijzeman, O. L. J.; van Zandvoort, M. M. J.; Labohm, F.; Vliegenthart, J. A.; Jongert, G. *J. Chem. Soc., Faraday Trans. 2* **1984**, *80*, 771.
(19) Erley, W.; Wagner, H.; Ibach, H. *Surf. Sci*. **1979**, *80*, 612.
(20) Kohn, W.; Sham, L. J. *Phys. Rev.* **1965**, *140*, 1133.
(21) Perdew, J. P.; Yue, W. *Phys. Rev. B* **1992**, *45*, 13244.
(22) Jacob, T.; Goddard, W. A. *J. Phys. Chem. B* **2004**, *108*, 8311.
(23) Zhang, Q. M.; Wells, J. C.; Gong, X. G.; Zhang, Z.; *Phys. Rev. B* **2004,** *69*, 205413.
(24) Riviére, P.; Busnengo, H. F.; Martin, F. *J. Chem. Phys*. **2004**, *121*, 751.
(25) Lai, W.; Xie, D. *Surf. Sci.* **2004**, *550*, 15.
(26) Feibelman, P. J.; Hammer, B.; Nørskov, J. K.;. Wagner, F.; Scheffler, M.; Stumpf, R.; Watwe, R. X.; Dumesic, J. *J. Phys. Chem. B* **2001**, *105*, 4018.
(27) Vanderbilt, D. *Phys. Rev. B* **1990,** *41*, 7892.
(28) Kresse, G.; Furthmüller, J. *VASP, The Guide*, Institut für Materialphysik, Univesität Wien: Wien, 2005.
(29) Monkhorst, H. J.; Pack, J. D. *Phys. Rev. B* **1976,** *13*, 5188.
(30) Doerr, M.; Frenking G. *Z. Anorg. Allg. Chem*. **2002**, *628*, 843.
(31) Petz, W.; Wellee, F.; Uddin, J.; Franking, G. *Organometallics* **1999**, *18*, 619.
(32) Sunderlin, L. S.; Wang, D.; Squires, R. R. *J. Am. Chem. Soc*. **1992**, *114*, 2788.
(33) Isaacson, A. D.; Truhlar, D. G. *J. Chem. Phys.* **1984,** *80*, 2888.
(34) Pelmenschikov, A. G.; Morosi, G.; Gamba, A.; Coluccia, S. *J. Phys. Chem. B* **1998,** *102*, 2226.
(35) Pacchioni, G.; Cogliandro, G.; Bagus, P. S. *Int. J. Quantum Chem*. **1992**, *42*, 1115.
(36) Mingfei, Z.; Lester, A.; Bauschlicher, C. W. *Chem. Rev*. **2001**, 101, 1931.
(37) Levine, I. N. *Quantum Chemistry*, 5th ed.; Prentice Hall: New York, 2000.
(38) Hill, T. L. *An Introduction to Statistical Thermodynamics*; Dover Publications: New York, 1986.
(39) Kittel, C.; Kroemer, H. *Thermal Physics*; W. H. Freeman: San Francisco, CA, 1980, Appendix E, p 460.
(40) Ramsey, N. F. *Phys. Rev.* **1956**, *103*, 20.
(41) Kein, M. J. *Phys. Rev.* **1956**, *104*, 589.